

Measurements on a Delta Wing in Unsteady Flow

A. G. Parker*

Texas A&M University, College Station, Texas

Low-speed wind-tunnel tests were undertaken to determine the vortex location, vortex burst location, and upper surface pressure distribution on a delta wing (aspect ratio = 2) in an oscillatory airstream. In steady flow an axisymmetric "tulip"-type burst was observed at all angles of attack, whereas in unsteady flow the vortex core gradually dissipated into turbulence for increasing angles of attack but formed a "helical"-type burst for decreasing angles. The pressure distributions showed that in unsteady flow there were considerable phase lags in the suction peaks associated with the vortices but virtually no lags elsewhere on the wing.

Nomenclature

| | |
|-----------|---|
| R | = aspect ratio |
| c_0 | = root chord |
| \bar{c} | = aerodynamic mean chord |
| c_p | = pressure coefficient |
| K | = reduced frequency parameter, $\omega \bar{c} / U$ |
| t | = time |
| U | = freestream velocity |
| x | = distance measured downstream from wing apex |
| α | = angle of attack |
| ω | = angular velocity |

Introduction

IN general, the steady flow past low-aspect-ratio (of order 1) delta wings with sharp leading edges is well understood and well documented.¹⁻¹⁵ Data on wings of aspect ratio 1.5 and above are considerably more scarce, and data for unsteady flow past these wings are virtually nonexistent.

The steady flow is characterized by two vortices, caused by leading-edge separation, which lie above the wing close to the leading edges. With increasing angle of attack these vortices increase in strength and move inboard causing two large suction peaks in the spanwise loading. At some point along their length the phenomenon of vortex breakdown, i.e., the bursting of the tightly rolled vortex core, occurs. For moderate angles of attack this is well downstream of the trailing edge, but with increasing angle the burst point moves rapidly forward until it occurs above the wing, producing unsteadiness in the loading.¹⁶⁻²² Increasing the aspect ratio causes the burst to reach the trailing edge at lower angles of attack.

Two distinct types of breakdown have been observed.^{17,18} One, more common at high Reynolds numbers, is an axisymmetric burst where the core suddenly expands to form a "tulip"-shaped "bubble." In the other, more generally seen at low Reynolds numbers, the core has a sharp kink and starts swirling in a helical path about its axis before breaking down into turbulence.

In unsteady flow the vortex cores move both laterally and vertically, and their loci have been measured during various motions for low-aspect-ratio wings.²³⁻²⁷ As yet, no effort has been made to ascertain the effect of flow unsteadiness on vortex bursting or to determine the effect of the burst on the transient loading. The current tests were planned to investigate these areas.

Equipment and Tests

Most of the work on delta wings in unsteady flow has been done by moving wings in a steady stream.²³⁻²⁷ Although the basic mechanics of this approach are straightforward, it does lead to problems with data acquisition and might not be representative of an aircraft entering a gust.

For the current tests, a thin sharp-edged delta wing, $R=2$, was mounted in the Texas A&M University 7 × 10 ft low-speed wind tunnel, and a stream oscillation device^{28,29} was used to produce a sinusoidal variation in flow angle of the airstream.

Frequencies of oscillation of 2 Hz and 4 Hz were used, and by setting the airspeed at 83.8 fps, reduced frequency parameters, $K = \omega \bar{c} / U$ of 0.2 and 0.4 were obtained at a Reynolds number (based on mean aerodynamic chord) of 1.3×10^6 . With these frequencies and tunnel speed the total wavelengths of the flow were 42 ft and 21 ft compared to the root chord length c_0 of 4 ft for the delta wing. The flow angle amplitude chosen for the tests was $\pm 8^\circ$ about a mean angle of attack of 15° .

The tests were divided into two sections, flow visualization and pressure measurements. For the flow visualization a liquid nitrogen and steam smoke generator developed at Texas A&M³⁰ was used to seed the vortex cores. Initially, the position of the vortex core and burst point in steady flow were determined, at several angles, by photography (Fig. 1). In the unsteady case photographs of the vortex locations at a particular time in a cycle were obtained by illuminating the flow with slave strobe lights triggered by the oscillatory flow drive motor (Figs. 2 and 3). From these photographs the loci of the vortex burst point vs angle of attack were determined (Fig. 4).

For the pressure measurements, 20 Validyne DP9 pressure transducers were mounted on the wing. One side of each transducer was connected to a port on the upper surface and the other side to a plenum referenced to freestream static

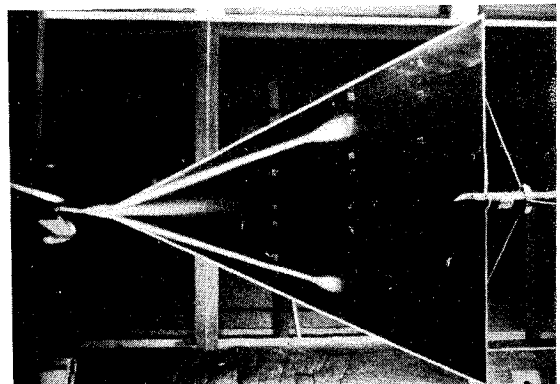
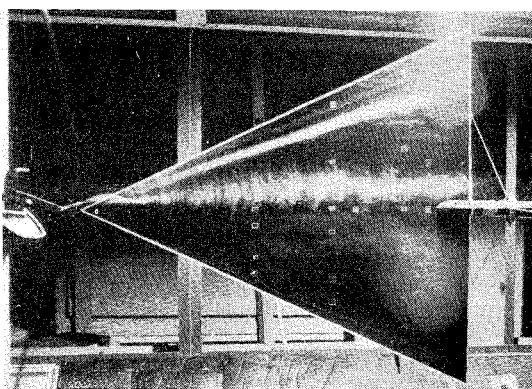
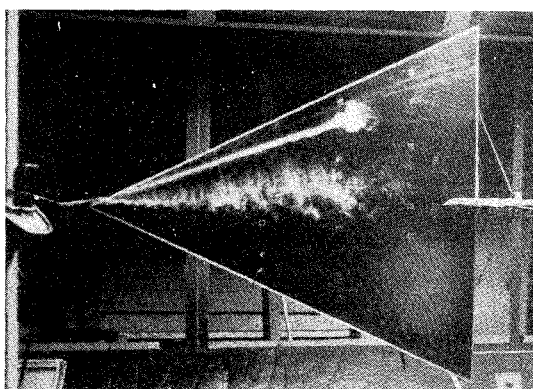
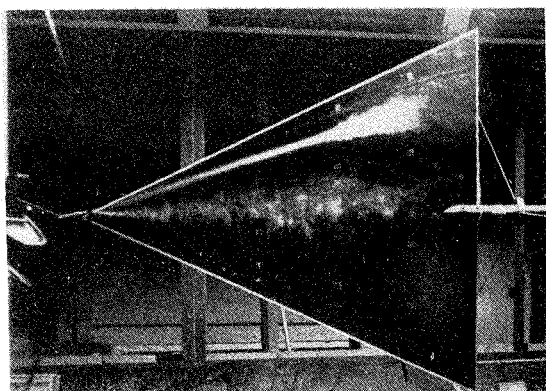
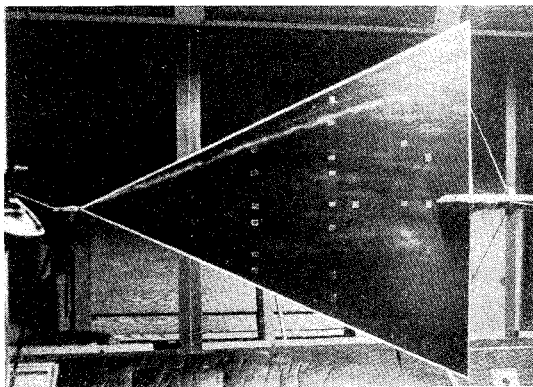
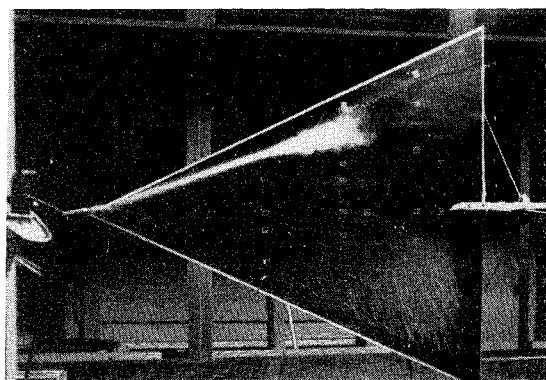
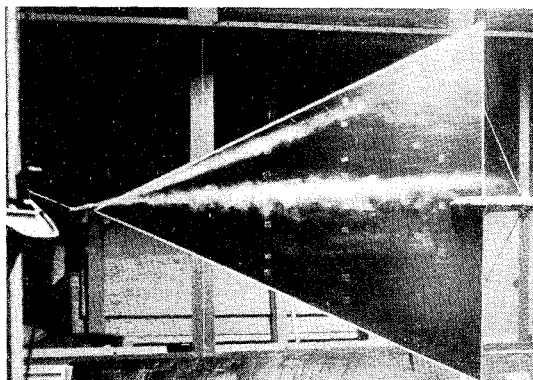
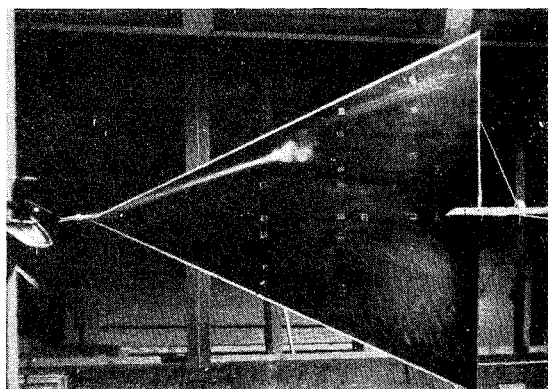
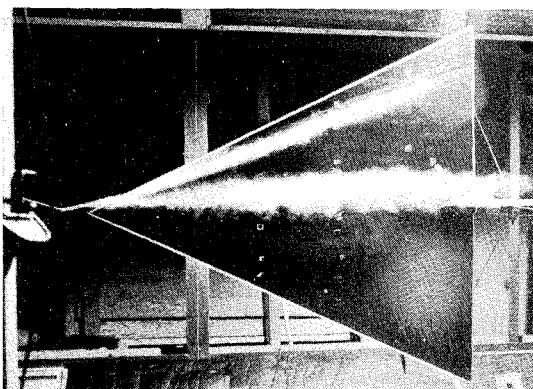


Fig. 1 Vortex flow visualization, steady flow $\alpha = 20^\circ$.

Received Sept. 2, 1975; revision received Aug. 12, 1976.

Index categories: Subsonic Flow; Nonsteady Aerodynamics; Jets, Wakes, and Viscid-Inviscid Flow Interactions.

*Assistant Professor, Aerospace Engineering Department. Member AIAA.

a) $\alpha = 15.3^\circ$ increasinge) $\alpha = 14.7^\circ$ decreasingb) $\alpha = 20.9^\circ$ increasingf) $\alpha = 9.1^\circ$ decreasingc) $\alpha = 23^\circ$ g) $\alpha = 7^\circ$ d) $\alpha = 20.5^\circ$ decreasingh) $\alpha = 9.5^\circ$ increasingFig. 2 Vortex flow visualization, unsteady flow $K = 0.2$.

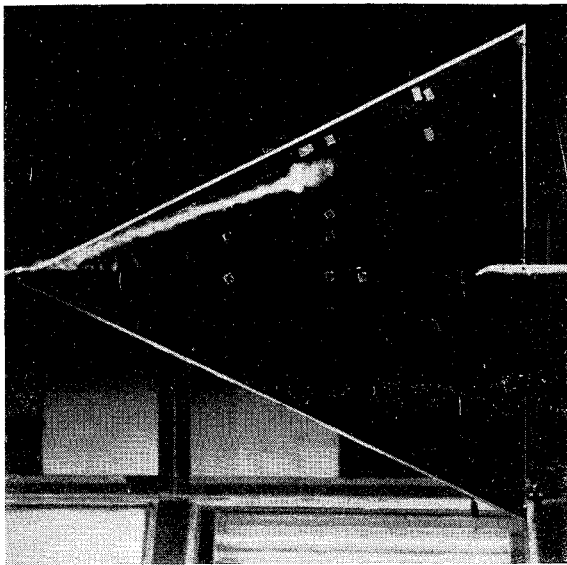


Fig. 3 Detail of a helical-type burst.

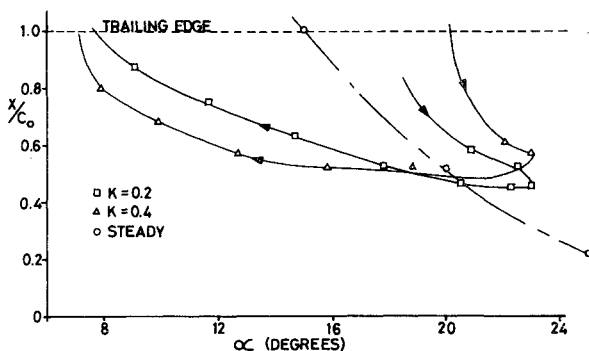


Fig. 4 Locus of vortex burst point vs angle of attack.

pressure. Outputs from all transducers, together with a signal indicating the flow direction, were recorded on Honeywell visicorders. After reduction, the load distributions on the wing were plotted at several angles of attack throughout a typical cycle at each frequency (Fig. 5).

Discussion

Flow Visualization

Steady Flow

At 5° angle of attack, α , in steady flow the vortices above the wing were weak, and it proved impossible to seed the cores adequately with smoke. When α was increased to 10° , the vortex core was well defined and easily seeded; toward the trailing edge the core tended to curve into the stream direction. Increasing α to 15° caused the cores to move inboard, and on one vortex the burst point moved up to the trailing edge, no bursting was evident in the other vortex. This asymmetry was probably caused by either a slight yaw angle on the wing or a disturbance to the flow caused by the smoke probe.

At 20° angle of attack (Fig. 1) the vortex cores had moved farther inboard and the burst points had moved forward to almost 50% of the root chord. These trends continued until at $\alpha = 30^\circ$ the burst points were at the 20% root chord position.

According to Sarpkaya¹⁸ the spiral type of vortex breakdown is the one more commonly observed over delta wings, and it was this type of burst that was observed by Maltby et al.²⁷ in a wind tunnel at Reynolds numbers of 1.5 to 6×10^6 ; however, in the current steady flow tests the burst was always of the axisymmetric "tulip" type which is consistent with the results of Lambourne,¹⁷ who pointed out that

his observations of the spiral-type burst were at very low Reynolds numbers in a water tunnel.

The position of the burst point as a function of angle of attack is plotted in Fig. 4. Numerically, the burst point in these tests at all angles of attack lies slightly ahead of Lambourne's measurements as expected for a slightly larger aspect ratio (2.0 as opposed to 1.86).

Oscillatory Flow

Photographs obtained at several angles of attack during oscillatory flow at $K=0.2$ are presented in Fig. 2. At 15.3° (Fig. 2a), with the angle of attack increasing, the vortex was still weak, and no burst occurred above the wing. At 20.9° (Fig. 2b), the vortex had moved inboard and burst at $x/c_0 = 0.6$. It should be noted, however, that this burst did not appear to be of the "tulip" type; rather the core expanded gradually, became turbulent and dissipated. By the time the maximum angle of attack had been reached (23° , Fig. 2c), the burst point had moved forward but still appeared to be of a gradual diffusion type. At 20.5° and decreasing (Fig. 2d), the burst point had not changed location but its character was changing. By the time α had decreased to 14.7° (Fig. 2e), the burst point had moved downstream and become a helical-type burst (see also Fig. 3). At 9.1° (Fig. 2f) the burst point was near the trailing edge of the wing and the vortex was decreasing in strength. As the angle passed through a minimum (Fig. 2g), the burst moved off the wing and the core moved outboard before moving inboard again with increasing angle ($\alpha = 9.5^\circ$, Fig. 2a).

The locus of the burst point throughout the cycle is plotted in Fig. 4. As the angle of attack increased to a maximum, the point of burst for $K=0.2$ significantly lagged the position in steady flow; also, the burst in oscillatory flow did not move as far forward as it did in steady flow. This is presumably because the wing was not at the maximum angle of attack long enough for the steady-state conditions to occur; the integrated vortex strength, which must affect the burst location, was always less in unsteady flow than it was at the maximum angle of attack in steady flow. As the angle of attack decreased from maximum, the position of the burst point in unsteady flow was aft of (i.e., leading) steady flow position until approximately $\alpha = 20.5^\circ$, when the steady and unsteady burst positions were coincident. With further decreases in angle, the unsteady results again lagged the steady data by increasing amounts. For $K=0.2$ the burst point finally moved off the wing at approximately 8° .

For $K=0.4$ the trends were similar to those observed at $K=0.2$, and a plot of the burst point vs angle of attack (Fig. 4) shows that, for increasing α , the burst position lagged both the steady and the $K=0.2$ cases up to maximum α . Then, unlike the $K=0.2$ data, the burst point continued to move forward as the angle of attack started to decrease and reached its maximum forward position when $\alpha = 21^\circ$; this maximum forward position was still downstream of the most forward position for $K=0.2$. As before, the burst location was in phase with the steady flow results at about 20° . As the angle of attack decreased further, the burst position lagged both the steady and the $K=0.2$ results and finally moved off the wing at about the minimum angle of attack.

Pressure Measurements

All of the pressure data obtained, both steady and unsteady, are presented in the form of carpet plots of the pressure coefficient c_p vs position at several angles of attack in Fig. 5.

With the wing at 15° angle of attack in steady flow (Fig. 5a), near the nose the two suction peaks were narrow and close to the leading edges; further downstream they moved slightly inboard, spread out, and decreased in magnitude due to the effects of secondary separation, indicated by the small peak outboard of the main vortex, and the Kutta condition of the trailing edge. In unsteady flow the distribution was

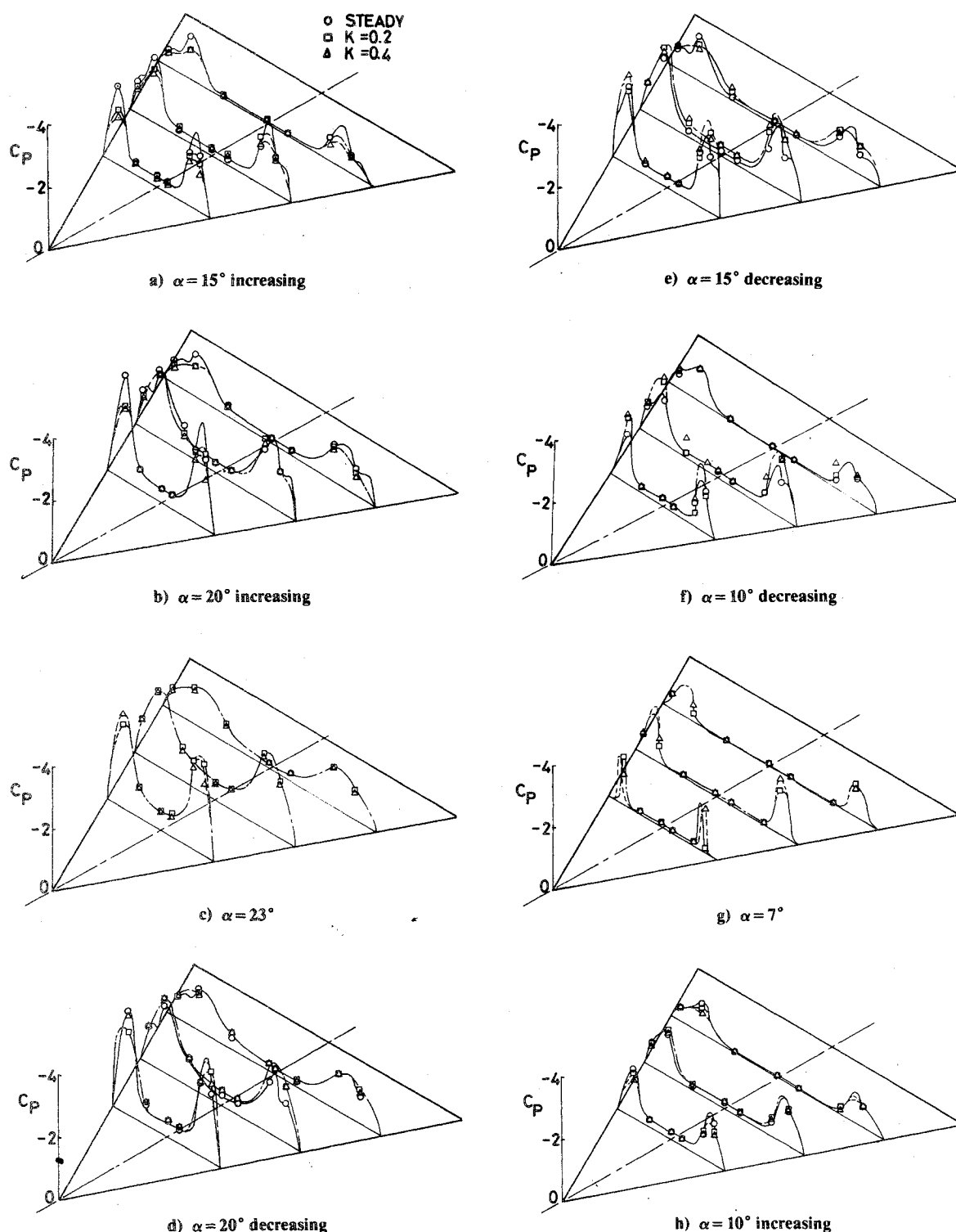


Fig. 5 Pressure distributions on a delta wing.

similar, but the peaks were slightly lower for $K=0.2$ and lower still for the $K=0.4$ case. These trends continued through $\alpha = 17.5^\circ$ until, at $\alpha = 20^\circ$ (Fig. 5b), it was true at the most forward measuring station ($x/c_0 = 0.4$), but at the midstation ($x/c_0 = 0.6$) the peaks in unsteady flow were slightly greater than in steady flow. A reason for this is probably in the vortex burst; flow visualization showed (Fig. 4) that at this angle of attack, in steady flow the burst occurred ahead of, whereas in unsteady flow, for α increasing, it had not reached $x/c_0 = 0.6$. Thus, in unsteady flow, full vortex suction still was being maintained. Peaks for $K=0.2$ were slightly higher than for $K=0.4$. At $x/c_0 = 0.8$ the peaks

for $K=0.2$ and 0.4 were about the same magnitude, the vortex had burst upstream of this location at $K=0.2$ but not for $K=0.4$, and the loss of suction due to bursting probably cancelled the loss due to phase lag.

By the time maximum angle of attack (23° , Fig. 5c) was reached, the vortex burst had moved ahead of $x/c_0 = 0.6$ for both frequency parameters, and the pressure distributions at $x/c_0 = 0.6$ and 0.8 were similar. The suction peaks at $x/c_0 = 0.4$, where no burst occurred in either case, were greater for the lower frequency.

By comparing the distributions at the various angles of attack, it can be seen that the total load on the wing increased

steadily as the angle of attack increased from 15° to 23° . When α decreased to 20° (Fig. 5d) the loading for all cases was similar, as might be expected since this is the angle at which the burst patterns were in phase. A major difference between the steady and unsteady data was that dips due to secondary separation apparent in the steady data were not present in the unsteady distributions; this might be caused by the ports being located at the "wrong" places to detect secondary separation in unsteady flow.

Again, little change in loading occurred as the angle of attack further decreased to 17.5° , but, by 15° (Fig. 5e) the load on the wing had started to decrease. An interesting point at this angle was distribution at $x/c_0 = 0.6$ and 0.8 , the suction peaks in unsteady flow were quite broad whereas they were narrow for steady flow. In steady flow at this angle vortex bursting did not occur until the trailing edge (Fig. 4), whereas, at $K=0.2$, it occurred at about $x/c_0 = 0.6$ and somewhat further forward for $K=0.4$, causing the peaks to become broader and lower.

As α decreased to 10° (Fig. 5f) the total lift continued to decrease. The vortex loading in unsteady flow at the two forward stations was considerably greater than for steady flow. At the rear station the vortex burst in unsteady flow caused the peaks to broaden and decrease in magnitude.

At the minimum angle of attack, $\alpha = 7^\circ$ (Fig. 5g), the vortex peak at $x/c_0 = 0.4$ for $K=0.2$ became very narrow and did not move as far outboard as the peak for $K=0.4$. The reason for this is not known, but it might be connected with a rapid collapse of the vortex core at low angles in large-amplitude oscillatory flow as discussed by Lowson.²⁴

As the angle of attack increased back up to 10° (Fig. 5h), the lift continued to decrease. It was not until 12.5° that the lift started to increase again.

In general, it can be seen that in oscillatory flow there was a phase lag, that increased with frequency, in the development of vortex lift. This was not so in the loading away from the influence of the vortices, i.e., along the center of the wing. Flow that came over the vortices and reattached along the centerline of the wing (the "potential" flow) responded fast enough so that there were no phase lags within the accuracy of measurement (except at high angles where the center section was influenced by the vortices). The phase lag that occurs in the vortex loading must occur because of the finite time it takes the vortex strength to change after a change in the leading-edge shedding rate; this is consistent with the measured lags in the locus of the burst points.

In the results presented here no wind-tunnel boundary corrections have been applied. Estimates for the magnitude of the angle-of-attack correction were made using standard steady flow values of lift coefficient, and these indicated that, at $\alpha = 7^\circ$ and 23° , corrections of order -0.2° and -0.6° would be needed. However, this type of correction cannot be justified rigorously in unsteady flow, so none have been applied.

Conclusions

On a sharp-edged delta wing of aspect ratio 2 in steady flow at Reynolds numbers of order 1×10^6 the vortex bursting was of the axisymmetric "tulip" type and the burst point moved upstream with increasing angle of attack. In unsteady flow ($\alpha = 15^\circ + 8 \sin \omega t$) this type of burst did not occur. As the angle of attack increased, the vortex core appeared to undergo a gradual viscous dissipation into turbulence; with decreasing angle, a helical (i.e., the vortex core swirls about its own axis) burst was observed. The locus of the burst point in unsteady flow lagged the steady position over most of the cycle. The burst point did not move as far forward in unsteady as in steady flow, probably because the vortex strength takes a finite time to build up and the leading-edge vorticity shedding rate was not maintained at the maximum value long enough for the vortex to reach equilibrium.

Measured pressure distributions indicated that the suction pressures due to the vortices in unsteady flow lagged behind

the steady-state pressures through most of the cycle whereas the loading in regions of "potential" flow remained in phase with the angle-of-attack variation, confirming that the vortices take a finite time to change strength after a change in angle of attack. Vortex bursting decreased the suction pressure and broadened the peak, causing a decrease in lift downstream of the burst. When the angle of attack was decreasing, the burst position in unsteady flow remained ahead of the steady-state position, causing a significant loss of lift over the rear of the wing.

Acknowledgment

This work was sponsored by the Office of Naval Research under Contract No. N00014-75-C-0255.

References

- ¹Parker, A. G., "Aerodynamic Characteristics of Slender Wings - A Review," *Journal of Aircraft*, Vol. 13, March 1976, pp. 161-168.
- ²Peckham, D. H., "Low Speed Wind Tunnel Tests on a Series of Uncambered Slender Pointed Wings with Sharp Edges," Royal Aircraft Establishment, Farnborough, England, Rept. Aer. 2613, 1958.
- ³Earnshaw, P. B. and Lawford, J. A., "Low Speed Wind Tunnel Experiments on a Series of Sharp Edged Delta Wings," Aeronautical Research Council, London, R&M 3424, 1964.
- ⁴Parker, A. G., "On Delta Wings in Unsteady Flow," Ph.D. Thesis, Queen Mary College, London University, 1970.
- ⁵Ornberg, T., "A Note on the Flow Around Delta Wings," *Kungl Tekniska Högskolan, Stockholm*, Aero TN 38, Feb. 1954.
- ⁶Hummel, D., "Zur Umströmung scharfkantiger schlanker Deltaflügel bei grossen Anstellwinkeln," *Zeitschrift für Flugwissenschaften*, Vol. 15, Oct. 1967, pp. 376-385.
- ⁷Polhamus, E. C., "Predictions of Vortex Lift Characteristics by a Leading-Edge Suction Analogy," *Journal of Aircraft*, Vol. 8, April 1971, pp. 193-200.
- ⁸Garner, H. C. and Lehrian, D. E., "Nonlinear Theory of Steady Forces on Wings with Leading-Edge Flow Separation," Aeronautical Research Council, London, R&M 3375, 1963.
- ⁹Mook, D. T. and Maddox, S. A., "Extension of a Vortex Lattice Method to Include the Effects of Leading-Edge Separation," *Journal of Aircraft*, Vol. 11, Feb. 1974, pp. 127-128.
- ¹⁰Brown, C. E. and Michael, W. H. Jr., "On Slender Delta Wings with Leading-Edge Separation," NASA TN 3430, 1955.
- ¹¹Mangler, K. W. and Smith, J. H. B., "Calculation of the Flow Past Slender Delta Wings with Leading Edge Separation," Royal Aircraft Establishment, Farnborough, England, Rept. Aero. 2593, 1957.
- ¹²Fink, P. J. and Taylor, J., "Some Early Experiments on Vortex Separation," Aeronautical Research Council, London, R&M 3489, 1966.
- ¹³Berndt, S. B., "Three Component Measurements and Flow Investigations of Plane Delta Wings at Low Speeds and Zero Yaw," *Kungl Tekniska Högskolan, Stockholm*, Aero. TN 4, 1949.
- ¹⁴Lambourne, N. C. and Bryer, D. W., "Some Measurements of the Positions of the Vortices for Sharp Edged Delta and Swept Back Wings," Aeronautical Research Council, London, Rept. 19,953, 1958.
- ¹⁵Marsden, D. J., Simpson, R. W., and Rainbird, W. J., "The Flow over Delta Wings at Low Speeds with Leading Edge Separation," College of Aeronautics, Cranfield, England, Rept. 114, 1957.
- ¹⁶Wentz, W. J. Jr. and Kohlman, D. L., "Wind-Tunnel Investigations of Vortex Breakdown on Slender Sharp Edged Wings," NASA CR 98737, Nov. 1968.
- ¹⁷Lambourne, N. C. and Bryer, D. W., "The Bursting of Leading Edge Vortices - Some Observations and Discussion," Aeronautical Research Council, London, R&M 3282, 1962.
- ¹⁸Sarpkaya, T., "An Experimental Investigation of the Vortex Breakdown Phenomena," Naval Postgraduate School, Monterey, Calif., Rept. NPS 59SL0071a, July 1970.
- ¹⁹Werle, H., "Sur l'éclatement des tourbillons d'apex d'une aile delta aux faibles vitesses," *La Recherche Aeronautique*, pp. 23-30.
- ²⁰Elle, B. J., "On the Breakdown at High Incidences of the Leading Edge Vortices on Delta Wings," *Journal of the Royal Aeronautical Society*, Vol. 64, 1960, p. 491.
- ²¹Earnshaw, P. B., "Measurements of Vortex Breakdown Position at Low Speed on a Series of Sharp-Edged Symmetrical Models," Royal Aircraft Establishment, Farnborough, England, TR 6407, 1964.

²²Bisplinghoff, R. L., Ashley, H., and Halfman, R. L., *Aerolasticity*, Addison Wesley, Reading, Mass., 1955, Chap. V.

²³Lambourne, N. C., Bryer, D. W., and Maybrey, J. F. M., "The Behavior of Leading Edge Vortices over a Delta Wing Following a Sudden Change of Incidence," Aeronautical Research Council, London, R&M No. 3645, March 1964.

²⁴Lowson, M. V., "The Separated Flows on Slender Wings in Unsteady Motion Communicated by Dr. J. P. Jones," Aeronautical Research Council, London, Rept. 24, 118, 1963.

²⁵Randall, D. G., "Oscillating Slender Wings in the Presence of Leading Edge Separation," Royal Aircraft Establishment, Farnborough, England, Structures Rept. 286, 1963.

²⁶Dore, B. D., "Calculations of the Transient Forces on Delta Wings," National Physical Laboratory, England, Aero Note 1033, 1965.

²⁷Maltby, R. L., Engler, P. B., and Keating, R. F. A., "Some Exploratory Measurements of Leading-Edge Vortex Positions on a Delta Wing Oscillating in Heave," Aeronautical Research Council, London, Rept. 3410, 1965, (with G. F. Moss).

²⁸Bicknell, J. and Parker, A. G., "A Wind-Tunnel Stream Oscillation Apparatus," *Journal of Aircraft*, Vol. 9, June 1972, pp. 446-447.

²⁹Parker, A. G. and Bicknell, J., "Some Measurements on Dynamic Stall," *Journal of Aircraft*, Vol. 11, July 1974, pp. 371-374.

³⁰Parker, A. G. and Brusse, J. C., "A New Smoke Generator for Flow Visualization in Low-Speed Wind Tunnels," *Journal of Aircraft*, Vol. 13, Jan. 1976, pp. 57-58.

From the AIAA Progress in Astronautics and Aeronautics Series

COMMUNICATION SATELLITE DEVELOPMENTS: SYSTEMS—v. 41

Edited by Gilbert E. LaVean, Defense Communications Agency, and William G. Schmidt, CML Satellite Corp.

COMMUNICATION SATELLITE DEVELOPMENTS: TECHNOLOGY—v. 42

Edited by William G. Schmidt, CML Satellite Corp., and Gilbert E. LaVean, Defense Communications Agency

The AIAA 5th Communications Satellite Systems Conference was organized with a greater emphasis on the overall system aspects of communication satellites. This emphasis resulted in introducing sessions on U.S. national and foreign telecommunication policy, spectrum utilization, and geopolitical/economic/national requirements, in addition to the usual sessions on technology and system applications. This was considered essential because, as the communications satellite industry continues to mature during the next decade, especially with its new role in U.S. domestic communications, it must assume an even more productive and responsible role in the world community. Therefore, the professional systems engineer must develop an ever-increasing awareness of the world environment, the most likely needs to be satisfied by communication satellites, and the geopolitical constraints that will determine the acceptance of this capability and the ultimate success of the technology. The papers from the Conference are organized into two volumes of the AIAA Progress in Astronautics and Aeronautics series; the first book (Volume 41) emphasizes the systems aspects, and the second book (Volume 42) highlights recent technological innovations.

The systematic coverage provided by this two-volume set will serve on the one hand to expose the reader new to the field to a comprehensive coverage of communications satellite systems and technology, and on the other hand to provide also a valuable reference source for the professional satellite communication systems engineer.

v. 41—Communication Satellite Developments: Systems—334 pp., 6 x 9, illus. \$19.00 Mem. \$35.00 List
v. 42—Communication Satellite Developments: Technology—419 pp., 6 x 9, illus. \$19.00 Mem. \$35.00 List

For volumes 41 & 42 purchased as a two-volume set: \$35.00 Mem. \$55.00 List

TO ORDER WRITE: Publications Dept., AIAA, 1290 Avenue of the Americas, New York, N.Y. 10019